Analysis and Optimal Design of Batch and Two-Column Continuous Chromatographic Frontal Processes for Monoclonal Antibody Purification

Ce Shi[a], Sebastian Vogg[b], Dong-Qiang Lin[a], Mattia Sponchioni[c], Massimo Morbidelli[d]*

a. Key Laboratory of Biomass Chemical Engineering of Ministry of Education, College of Chemical and Biological Engineering, Zhejiang University, Hangzhou 310027, China

b. YMC ChromaCon, Technoparkstrasse 1, 8005 Zürich, Switzerland

c. Department of Chemistry, Materials and Chemical Engineering "Giulio Natta", Politecnico di Milano, Via Mancinelli 7, 20131 Milano, Italy

d. Institute for Chemical and Bioengineering, Department of Chemistry and Applied Biosciences, ETH 11 Zurich, Vladimir-Prelog-Weg 1-5/10, 8093 Zürich, Switzerland

1. Introduction

The increasing market share of monoclonal antibodies (mAbs), with 10% annual growth and more than 70 formulations approved in the last decade, makes mAbs one of the most important classes of biopharmaceuticals today[1-5]. The increasing number of therapeutic indications and the emerging of biosimilars contribute to strengthen the

23   demand for safe, efficient and cost effective manufacturing processes[6,7]. Continuous

24   integrated bioprocessing indeed goes in this direction[8-10] and it is therefore encouraged

25   by regulatory authorities [11,12].

26   Frontal chromatography has seen increased interest for protein purification, in

27   particular as a polishing step in downstream processes for therapeutic proteins

28   production, as for example in the purification of monoclonal antibodies (mAbs) from

29   high molecular weight impurities, e.g., aggregates, using cation exchange resins[13-17].

30   The schematic diagram of frontal chromatography operated on a single (batch) column

31   is shown in Figure 1a. Here, the eluate from the capture step (feed), containing both the

32   monomer and the aggregates, is first loaded into the column. The impurity (aggregates)

33   binds stronger to the cation exchange resin and displaces the weaker binding product

34   (monomer), which thus elutes first and is collected in the product pool. Loading is

35   continued until reaching, in general, sufficiently high purity in the pool and relatively

36   high recovery (yield). Next, a washing step is applied to recover the residual monomer

37   still present in the column into the product pool, so as to further increase the yield, but

38   being careful not to elute also the aggregates, which would spoil the purity below

39   specifications. Finally, regeneration and re-equilibration (RR) are carried out to elute

40   all the impurities (and remaining product) into the waste and prepare the column for the

41   next loading step.

42   In such a batch operation, the loading time and linear velocity have to be properly

43   selected so as to process the largest amount of material, without letting too much

44   aggregate into the product pool, so as to preserve purity. In the following washing step,

45 the linear velocity and duration should be carefully chosen to elute as much as possible

46 of the remaining product, thus maximizing the yield, while not desorbing the impurity

47 beyond the purity specification [18]. Therefore, batch frontal chromatography suffers

48 from an intrinsic purity-yield tradeoff. High loadings and harsh washing conditions

49 enable the recovery of much of the product, and thus an improved monomer yield, but

50 an overall low purity. On the other hand, low loadings and too mild washing conditions

51 enable high purity of the pool but prevent full recovery of the product, at the expense

52 of the process yield.

53   In order to alleviate this purity-yield tradeoff, a novel cyclic two column

54 continuous chromatographic process (referred to as Flow2) has been developed [18]. The

55 schematic diagram is illustrated in Figure 1b. This is a periodic process, where each

56 switch is constituted of three steps, after which the two columns exchange their role. In

57 the first step, the two columns are fed while being interconnected, so that the

58 breakthrough of the aggregates from the first column is captured by the second column.

59 In the next interconnected washing step, with inline dilution between the two columns,

60 both the product and the unbound impurity left in the first column are eluted into the

61 second column. With the proper inline dilution, both of them are bound in the second

62 column. Finally, in the third step, the two columns are disconnected. The first one

63 undergoes the RR process while the second one is loaded with the fresh feed.

64   With two columns interconnected during loading and the following washing with

65 inline dilution, aggregates are prevented from eluting from the second column into the

66 product pool and more monomer can be eluted from the first column, thus improving

67   the tradeoff between purity and yield. In addition, the washing conditions (buffer and

68   duration) do not need to be carefully designed as in the case of batch operation, thus

69   increasing the process robustness. However, the design of this cyclic process needs to

70   account for the increased number of operational parameters and complexity of the

71   process dynamics, which can be best achieved using model-based approaches [19-24].

72   In this work, the fundamental aspects of batch and continuous frontal

73   chromatography are analyzed. A model-based optimal design procedure, valid for both

74   batch and Flow2 processes, is developed with reference to three process performance

75   parameters: yield (recovery), purity and productivity. In particular, Pareto Fronts of

76   productivity and yield, with purity fixed at given specification values (P_{spec}), computed

77   based on reliable chromatographic models of the two processes, are discussed. Next,

78   the two processes, each operated at its own optimal conditions, are compared. This

79   analysis is conducted with reference to the polishing of a mAb of industrial relevance

80   and accounts, in addition to yield, purity and productivity [25], also for the important

81   concept of process robustness, which is a major concern particularly in

82   biopharmaceutical applications [26,27]. This has been quantified using a rigorous model-

83   based sensitivity analysis of the process performance with respect to its operating
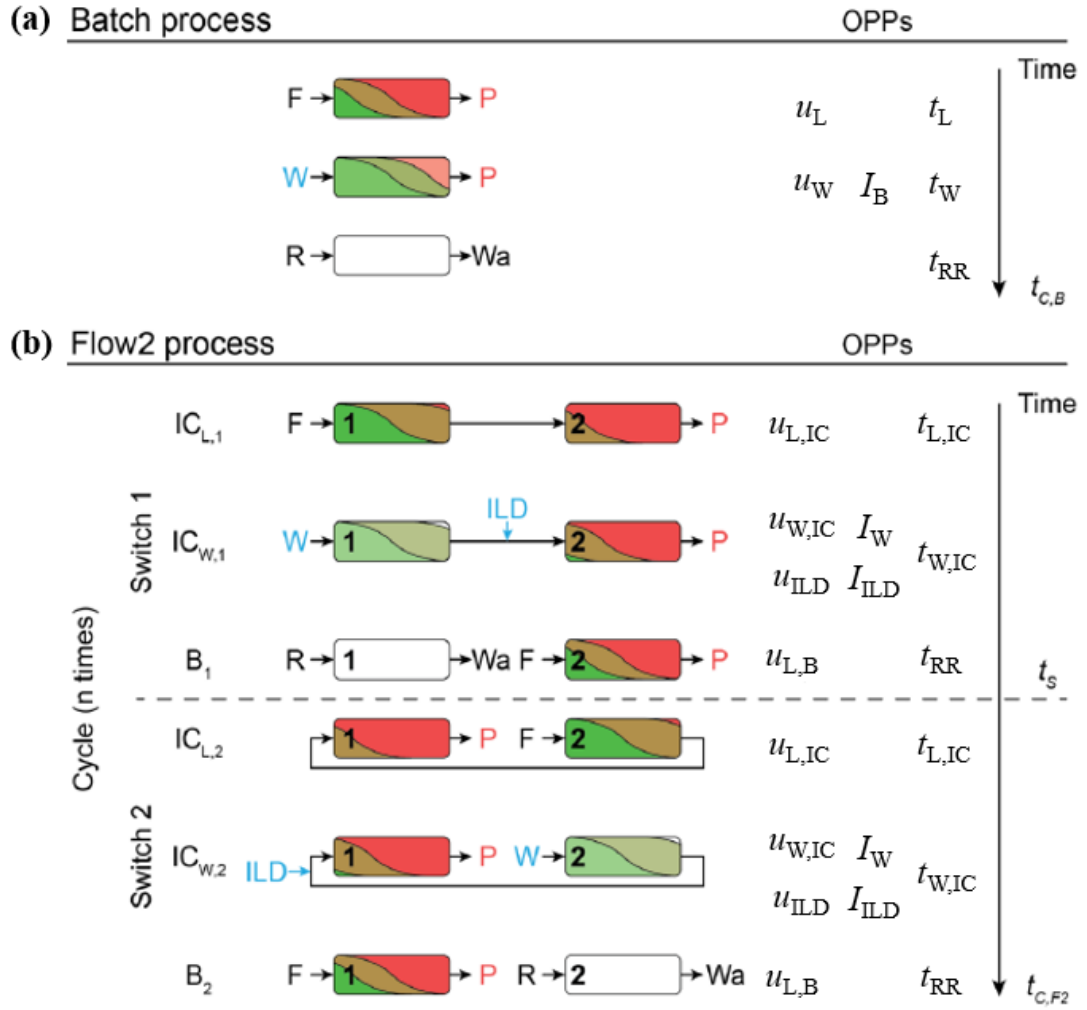
84   process parameters.

Figure 1. Schematic diagram of batch frontal chromatography (a) and continuous

Flow2 processes (b)[18].

2. Model-Based Optimal Design Methods

2.1 The Chromatographic Model

The chromatographic lumped kinetic model with linear driving force approximation has been used in all simulations [16,28,29]:

$$\frac{\partial c_i}{\partial t} = -\frac{u_{sf}}{\varepsilon_{t,i}} \frac{\partial c_i}{\partial x} + \frac{u_{sf}}{\varepsilon_{t,i}} d_{ax,i} \frac{\partial^2 c_i}{\partial x^2} - \frac{1-\varepsilon_{t,i}}{\varepsilon_{t,i}} \frac{\partial q_i}{\partial t} \tag{1}$$

$$\frac{\partial q_i}{\partial t} = k_{m,i}(q_i^{eq} - q_i) \tag{2}$$

95   with i = M, A and the boundary conditions:

96   $$c_i(x, t = 0) = 0$$

97   $$c_I(x, t = 0) = I_0$$

98   $$c_{pH}(x, t = 0) = pH_0$$

99   $$c_i(x, t = 0) = c_{i,in}(t) + d_{ax,i} \frac{\partial c_i}{\partial x}\Big|_{x=0}$$

100 $$\frac{\partial c_i}{\partial x}\Big|_{x=L_{col}} = 0$$

101 The mixing node in the continuous process has been simulated as follows:

102 $$c_{i,in,col2} = \frac{c_{i,in,col1} u_{W,IC} + c_{i,ILD} u_{ILD}}{u_{W,IC} + u_{ILD}} \tag{3}$$

103 The adsorption equilibrium has been described through a surrogate model, which

104 mimics the behavior of the DLVO-derived model, based on the competitive Langmuir

105 isotherm and appropriate empirical correlations [18,30] as follows:

106 $$q_i^{eq} = \frac{H_i c_i}{1 + \sum_j \frac{H_j c_j}{q_j^{sat}}} \tag{4}$$

107 $$q_i^{sat} = a_i^{sat} pH + b_i^{sat} \tag{5}$$

108 $$H_i = \alpha_i I^{-\beta_i} \tag{6}$$

109 $$\log_{10} \alpha_i = a_i^\alpha pH + b_i^\alpha \tag{7}$$

110 $$\beta_i = a_i^\beta pH + b_i^\beta \tag{8}$$

111 The meaning of all variables and parameters is explained in the notation section,

112 while the parameter values adopted in the simulations are listed in Table 1.

113

114

115

6

116 *Table 1. Values of the chromatographic model parameters* [18]

	Parameter	Unit	Salt	Monomer	HMW
d_{col}	Column diameter	cm	--------------------0.5--------------------		
L_{col}	Bed height	cm	--------------------5--------------------		
ε_b	Bed porosity	-	--------------------0.39--------------------		
$\varepsilon_{t,i}$	(Accessible) total porosity	-	0.95	0.65	0.65
$\varepsilon_{p,i}$	(Accessible) particle porosity	-	0.93	0.43	0.43
a_i^{Sat}	Slope of q_i^{Sat} vs. pH	-	n/a	0	0
b_i^{Sat}	Intercept of q_i^{Sat} vs. pH	-	n/a	212	106
a_i^{α}	Slope of $\log_{10}\alpha$ vs. pH	-	n/a	-1.270	-3.090
b_i^{α}	Intercept of $\log_{10}\alpha$ vs. pH	-	n/a	31.22	46.90
a_i^{β}	Slope of β vs. pH	-	n/a	1.128	0.676
b_i^{β}	Intercept of β vs. pH	-	n/a	5.227	9.870
$d_{ax,i}$	Axial dispersion coefficient	cm	0.034	37	98
$k_{m,i}$	Mass transfer coefficient	1/min	170	1.3	0.53

117 **2.2 Process performance parameters**

118   As mentioned above, the process performance is quantified in the following using

119 three process performance parameters: the productivity, *Pr* of the target species, i.e.,

120 mAb, defined as:

121 $$Pr = \frac{m}{n_{col}V_{col}t_C} \tag{9}$$

122 where *m* is the mass of target recovered in the product pool in one cycle of duration t_C

123   using n_{col} columns, each with volume V_{col}, the yield, Y of the target protein defined as:

124
$$Y_i = \frac{m}{m_{load}} \tag{10}$$

125   where m_{load} is the amount of target protein loaded on the column in one cycle, and the

126   purity, P defined as:

127
$$P = \frac{m}{\sum_i m_i} \tag{11}$$

128   where the sum at the denominator is extended to the mass m_i of all proteins present in

129   the product pool.

130   **2.3 Optimization methods**

131   The optimal design of frontal chromatographic processes can be complex. For this,

132   a specific procedure has been devised, based on a series of suitable steps, and referred

133   to as the *design procedure* (DP) in the following. This allows to facilitate and guarantee

134   the identification of the optimal operating conditions, for a given set of performance

135   parameters. The obtained results are compared with corresponding results obtained by

136   a multi-objective optimization procedure based on Genetic Algorithms [31].

137   The general concept of the design procedure is based on the evaluation of the

138   loading and washing times (see Figure 1), which describe the Pareto Front of

139   productivity and yield at a given purity equal to the specification value, $P_{spec.}$ The

140   regeneration and re-equilibration time, t_{RR} (Figure 1) is expected to derive from a

141   specifically designed experimental study conducted on a single column and is therefore

142   considered as a given value in this work. The basic idea is to first compute, all the other

143   parameters and operating conditions being fixed, the loading times leading to purity

144   values at the end of the first loading step, P_1 ranging from 100% to P_{spec}. In the

145   following washing step, the process purity can only decrease and the corresponding

146   duration is computed such that, for each one of the previous P_1 values, it leads to the

147   required purity P_{spec}. For each pair of loading and washing time values, we then

148   compute the corresponding productivity and yield values, being in all cases the purity

149   equal to P_{spec}. At this point, we can order all the obtained values in a productivity versus

150   yield plot and obtain the desired Pareto Front at fixed purity. This procedure can be

151   repeated by changing any other of the relevant parameters, like the buffer compositions

152   or the column or particle size, and compute the new Pareto Front. This approach is

153   useful not only to find the optimal operating conditions of the process, but also to

154   quantify the robustness of a given process design, as well as the economic impact of

155   the different operating conditions.

156   Alternatively, the optimization problem can be approached as a whole, without

157   attempting any problem decomposition, using a fully general multi-objective

158   optimization algorithm. The function 'Gamultiobj' of the MATLAB library [32], based

159   on a Genetic Algorithm, has been used in this work and the obtained results are

160   compared with those of the *ad-hoc* design procedure.

161   In the next section, we describe in detail the algorithm to compute the optimal

162   loading and washing times described above for both the batch and the Flow2 processes.

163

164   **3. Optimal Design of Frontal Chromatography Processes**

165   **3.1. The Batch Process**

166   The Pareto Front of productivity and yield with constant fixed P_{spec}, computed

167 with both methods, are compared first in the case of a batch process. All parameters,

168 unless otherwise specified, are kept constant at the values summarized in Table 2.

169

170 *Table 2. Batch Operating Conditions*

Parameters	Unit	Value
$c_{L,mono}$	g/L	4.5
$c_{L,agg}$	g/L	0.5
I_L	mM	80
I_W	mM	120
I_{RR}	mM	1000
pH_L	-	5
pH_W	-	5
pH_{RR}	-	5
u_L	cm/hr	300
u_W	cm/hr	300
u_{RR}	cm/hr	300
t_{RR}	min	15

171

172 With illustrative purposes, the requested purity the value was set as $P_{spec} = 99\%$. The

173 procedure develops according to the following three steps:

174 *Step 1: Compute the purity values at the column outlet, P_1 during the loading phase*

175 *(Figure 1a) for increasing loading time values, t_L.*

176   As t_L increases, first the product breaks through from the outlet of the column into

the product pool, followed by the impurity at longer times, thus reducing the purity in

the product pool, P_1, as shown in Figure 2a. As the loading proceeds the purity

decreases from 100% until $P_1 = P_{spec}$, which indicates the maximum acceptable value

of t_L. In this conditions, in fact, the washing time in the next step should be set to zero

to avoid any further decrease in purity below specification, but of course this would not

allow for any improvement in the process yield. Accordingly, at optimal operation, the

value of t_L should be shorter than 72 min, which corresponds to P_1 values ranging from

100% to the $P_{spec} = 99\%$ value.

Step 2: For each of these pairs of values t_L and P_1, compute the corresponding washing

time, t_w, which, starting from P_1, leads to a final purity, P equal to P_{spec}.

The obtained process yield and purity values are shown in Figure 2b as a function

of the washing time, t_W, as an example for the case of t_L=60 min and P_1=99.5%. It is

seen that the process purity, P decreases while Y increases for increasing washing times.

The decrease in the process purity is because more eluate, including both product and

impurity, is washed out into the product pool. On the other hand, the yield increases

when increasing t_W since more product is recovered. By selecting the purity value equal

to P_{spec}, the corresponding values of the yield, $Y_{P=P_{spec}}$ and the washing time, $t_{W,P=P_{spec}}$

are found.

Step 3: Repeat the procedure above to calculate productivity, Pr and yield, Y for each

of the pairs of values t_L and P_1 in Figure 2a and derive the corresponding Pareto Front

at fixed purity equal to P_{spec}.

Using the t_L and P_1 values in Figure 2a, the curve shown in Figure 2c is obtained,

representing the yield as a function of the washing time leading to process purity, $P =$

99%. On the other hand, it is seen that the corresponding productivity values, computed

through equation (19), decrease with t_{wash}, leading to the trade-off between Pr and Y

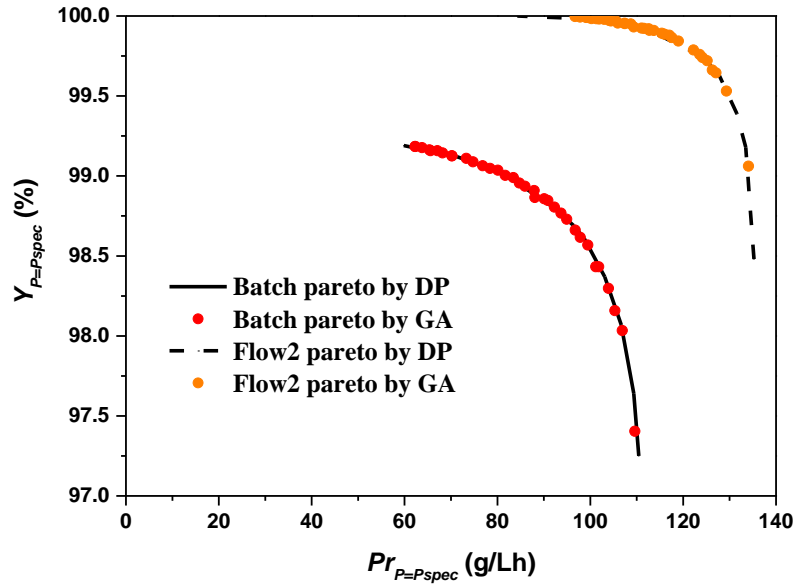illustrated by the Pareto Front, with fixed purity P_{spec}, in Figure 3.

Figure 2. The design procedure for the batch and Flow2 proesses. (a) Batch P_1 as a

function of the loading time; the bar indicates P_{spec} (b) Batch P and Y as a function of

the washing time at $t_L=60$ min and $P_1= 99.5\%$ (c) The relationship between $Y_{P=Pspec}$

and $Pr_{P=Pspec}$ as a function of $t_{W,P=Pspec}$ for a batch process. (d) Flow2 P_2 as a function

of the loading time, $t_{L,total}$; the bar indicates P_{spec} (e) Flow2 P and Y as a function of the

washing time at $t_{L,total} = 70$ min and $P_2=99.8\%$ (f) The relationship between $Y_{P=Pspec}$

210   *and $Pr_{P=Pspec}$ as a function of $t_{W,P=Pspec}$ for a Flow2 process.*

211

212   The results of the *ad-hoc developed design procedure* (DP) are compared with

213   those of a general multiobject Genetic Algorithm (GA), using 50 individuals per

214   generation and a maximum of 200 generations. The purity constraint has been

215   introduced by imposing heavy penalties on purity values smaller than P_{spec}. At each

216   iteration, the 35 fittest individuals are selected to plot the Pareto Front and produce the

217   next generation. The GA optimization is terminated when the 200th generation is

218   reached or when the average relative change in the best fitness function value, with

219   respect to the previous generation, is less than or equal to the function tolerance (10^{-4}).

220   The performance values corresponding to the best 35 individuals in the last generation

221   are compared with the Pareto Front computed through the design procedure in Figure

222   3. It is seen that all the points corresponding to the GA optimization are on or slightly

223   below the curve generated by the design procedure, indicating that the two methods

224   provide essentially the same result. In addition, it is found that all the points obtained

225   through the GA method exhibit a purity value equal to the constrain value of 99% with

226   a maximum 1 % relative deviation.

227   It is worth noticing that, although the two methods give equivalent results, the

228   associated computational effort is quite different. In the *design procedure*, only 35*10

229   objective functions are calculated: 35 for getting the Pareto Front, and 10 each for

230   determining the t_W values corresponding to 99% purity. On the other hand, in the multi-

231   objects GA optimization, 50*200 functions are calculated: one each for the 50

232   individuals constituting each of the 200 generations.

Figure 3. Pareto Front of Pr and Y computed with the design procedure (DP)

compared with the results of the global optimization based on genetic algorithm (GA),

for P_{spec} = 99% and other parameter values as in Tables 1, 2 and 3.

3.2 The Continuous Flow2 Process

The two optimization methods considered above have been developed and compared also for the Flow2 process. In particular, we optimize the interconnected loading and washing times, $t_{L,IC}$ and $t_{W,IC}$ (Figure 1b) in order to obtain the Pareto Front of productivity, *Pr* and *Y* with fixed purity equal to P_{spec}. Note that in this process, the batch loading time is fixed and equal to the regeneration and re-equilibration time, t_{RR}, which is considered as a given constant in this analysis (Figure 1b). Accordingly, the total loading time given by $t_{L,total}$ = t_{RR} + $t_{L,IC}$, can actually be changed only through the interconnected loading time, $t_{L,IC}$. All remaining parameters are kept constant and equal

14

247   to the values summarized in Tables 1 and 3. It is to be noted that all the simulation

248   results reported for the continuous Flow2 process refer to steady state conditions. These

249   are obtained by simulating the entire dynamics of the process and considering the

250   transient behavior completed when the mass flow of each protein entering and leaving

251   differ for no more than 1.0 % , which means that no protein is accumulated or lost in

252   the system during every switch.

253   *Table 3. Flow2 Operating Conditions*

Parameters	Unit	Value
$c_{L,\,mono}$	g/L	4.5
$c_{L,\,agg}$	g/L	0.5
I_{IC}	mM	80
I_{W}	mM	120
I_{ILD}	mM	10
I_{RR}	mM	1000
$pH_{L,IC}$	-	5
$pH_{W,IC}$	-	5
pH_{ILD}	-	5
pH_{RR}	-	5
$u_{L,IC}$	cm/hr	300
u_{W}	cm/hr	300
u_{ILD}	cm/hr	300
u_{RR}	cm/hr	300

t_{RR}	min	15

254

255   As mentioned above, differently from the batch process, the Flow2 process has two

256   loading phases within one switch: interconnected and batch loading. In the following,

257   we consider these two steps together with a total duration, $t_{L,total} = t_{RR} + t_{L,IC}$, with a

258   purity value P_2, which is analogous to the purity P_1 in the batch process. After the

259   washing step, the product purity is indicated as P which represents the final product

260   purity at the end of the switch as indicated in Figure 1b.

261   The design procedure in this case is organized as follows:

262   *Step 1: Simulate the process for changing total loading times, $t_{L,total}$ so as to obtain*

263   *purity values, P_2 ranging from 100% to the requested P_{spec}=99%.*

264   As shown in Figure 2d, the obtained P_2 values decrease as a function of the loading

265   time, $t_{L,total}$: starting from 100% to values below the imposed process purity

266   specification, P_{spec}, which is reached at $t_{L,total} = 78$ min.

267   *Step 2: For each pairs of values $t_{L,total}$ and P_2 in Figure 2d, with $P_2 > P_{spec}$, compute the*

268   *interconnected washing time ($t_{W,IC}$ in Figure 1b) leading to a product purity, P at the*

269   *end of the switch equal to the requested P_{spec}.*

270   As an example, Figure 2e shows the results obtained for the pair of values $t_{L,total} = 70$

271   min and P_2 =99.8%. As expected, it is seen that as the washing time increases, the purity

272   decreases while the yield increases. The values $Y_{P=P_{spec}}$ and $t_{W,P=P_{spec}}$, corresponding to

273   the requested purity value P_{spec}, can be obtained.

274   *Step 3: Repeat the previous step for each of the pairs of values P_2 and $t_{L,total}$ in Figure*

275   *2d and with the corresponding productivity, Pr and yield, Y values derive the*

276　*corresponding Pareto Front, at fixed purity equal to P_{spec}.*

277　　　Repeating the step above for all the pairs of values P_2 and $t_{L,total}$ in Figure 2d, the

278　maximum yield values for each washing time, t_W, compatible with the fixed purity, P_{spec}

279　can be computed as shown in Figure 2f. From these, and the corresponding productivity

280　values, Pr computed through Equation 9, the Pareto Front for productivity and yield at

281　fixed purity equal to P_{spec} in Figure 3 is obtained.

282　　　The latter is compared in the same firgure with the corresponding Pareto Front for

283　the batch frontal chromatography process, obtained as discussed above. The higher

284　efficiency of the Flow2 process, which will be discussed later in more detail, is clearly

285　indicated by the movement of the Pareto Front to the upper right corner of the figure.

286　　　As mentioned above, the multi-object global optimization of the Flow 2 process

287　has also been performed based on a genetic algorithm, using 50 individuals per

288　generation and a maximum of 300 generations. The obtained results, corresponding to

289　the 35 best individuals in the last generation, are shown by the points shown in Figure

290　3 and compared with the results of the ad-hoc design procedure. It is seen that the two

291　methods provide equivalent results, although the GA approach requires a significantly

292　larger computational effort, as already discussed in the context of the batch process.

293

294　**4. Analysis and Comparison of Optimized Batch and Flow 2 Process Performance**

295　　　A general difficulty when comparing different processes, and not only in

296　chromatography, is to select "fair" conditions for the comparison, that is operating

297　conditions that do not favor one or the other. In this work, we consider each process

under independently optimized operating conditions. In particular, we are going to analyze the behavior of batch and Flow 2 processes as a function of operating parameters which are known to be most relevant in chromatography, such as linear velocities in the columns and composition of the loading and washing buffers. In all cases, we consider for each process the optimal Pareto yield-productivity (with fixed purity, P_{spec}) obtained by optimizing the durations of both the loading and washing steps. In the following, the design procedure developed in this work will be used, since we have shown that this provides the same results as a general multi-objective optimization, but with lower computational effort. The objective is to analyze and compare the behavior of each of such processes with respect to both process performance and robustness.

4.1 The relevant performance parameters

Among the various chromatographic steps involved in the production of mAbs, frontal chromatography is a quite promising candidate for the polishing step after protein capture, where high purity, productivity and robustness are requested. For example, in the case of aggregate removal, mAb purity values well above 95% are typically needed. In Figure 4, the tradeoff between productivity and yield for optimal batch process operations at specification purities, P_{spec} equal to 95%, 98% and 99% is shown. It can be seen that more stringent purity constraints move the Pareto Front to the lower left corner with correspondingly lower values for both productivity and yield. It can also be seen that the yield is always higher than 98%, indicating that this is not the discriminating performance parameter in designing frontal chromatography

320   processes. Accordingly, in the following we will base the process comparison on the

321   tradeoff between yield and productivity as well as on the operation robustness, with a

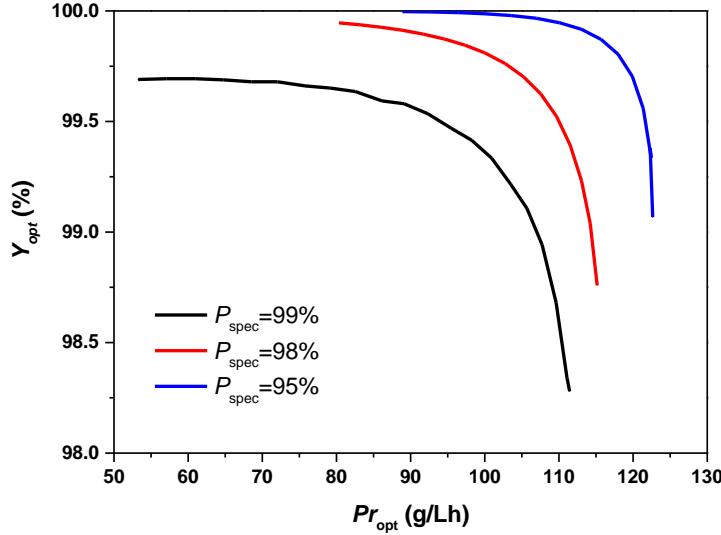322   stringent purity specification of $P_{spec} = 99\%$..

Figure 4. Tradeoff between yield and productivity (Pareto Front) for the batch process

at various P_{spec} values. Operating contitions as in Tables 1 and 2.

4.2 Role of linear velocities in loading and washing

In this section, the effect of the liquid velocity during loading and washing is

analyzed in both Batch and Flow2 process. The values considered range from 300 cm/hr

to the value compatible with the maximum pressure drop tolerated by the stationary

phase as computed through the Blake-Kozeny equation [33]

$$\frac{\Delta P}{L_{col}} = \frac{150\mu}{d_p^2} \frac{(1-\varepsilon_b)^2}{\varepsilon_b^3} u_{sf} \tag{12}$$

Considering the maximum pressure drop equal to 0.15 MPa[34], the maximum linear

velocity of 3000 cm/hr is obtained for the 5 cm bed height and 50 μm particle radius

335   considered in this work. The values of the remaining operating parameters used in all

336   simulations considered in the following are listed in Tables 1 to 3.

4.2.1 Batch process

338   The effect of loading and washing velocities is analyzed first with u_L changing

339   from 300 to 3000 cm/hr with fixed u_W = 300 cm/hr, and then with u_W changing from 1

340   to 3000 cm/hr with fixed u_L = 300 cm/hr. The Pareto fronts obtained for various u_L

341   values are shown in Figure 5a. Note that, in general, the Pareto fronts do not necessarily

342   cover the entire range of possible yield and productivity values, since some portions of

343   them may not be achievable with the considered operating conditions. In particular, it

344   is seen that as the loading velocity increases, the process performance first improves,

345   with the Pareto moving to the right of the plot, thus enabling higher productivity values

346   for a given recovery value. This is because at higher loading velocity the loading time

347   is shortened to the benefit of productivity. However, when further increasing the loading

348   velocity, intraparticle mass transfer becomes more and more limiting [35,36], leading

349   eventually to the earlier breakthrough of the impurities and then to lower purity values.

350   This explains the worsening of the Pareto front at 3000 cm/hr with respect to lower

351   loading velocities in Figure 5a. The effect of the washing velocity is showed in Figure

352   5b. It is seen that as the washing velocity increases from 300 to 900 cm/hr, the Pareto

353   front extends to higher productivities, but it decreases again for further increasing u_W

354   values. For the maximum allowable washing linear velocity of 3000 cm/hr, the process

355   performance is in fact inferior to all the other washing velocities in almost the entire

356   range of operating conditions. Limiting intraparticle mass transfer prevails at such

washing linear velocity, so that more target protein remains in the column, and both
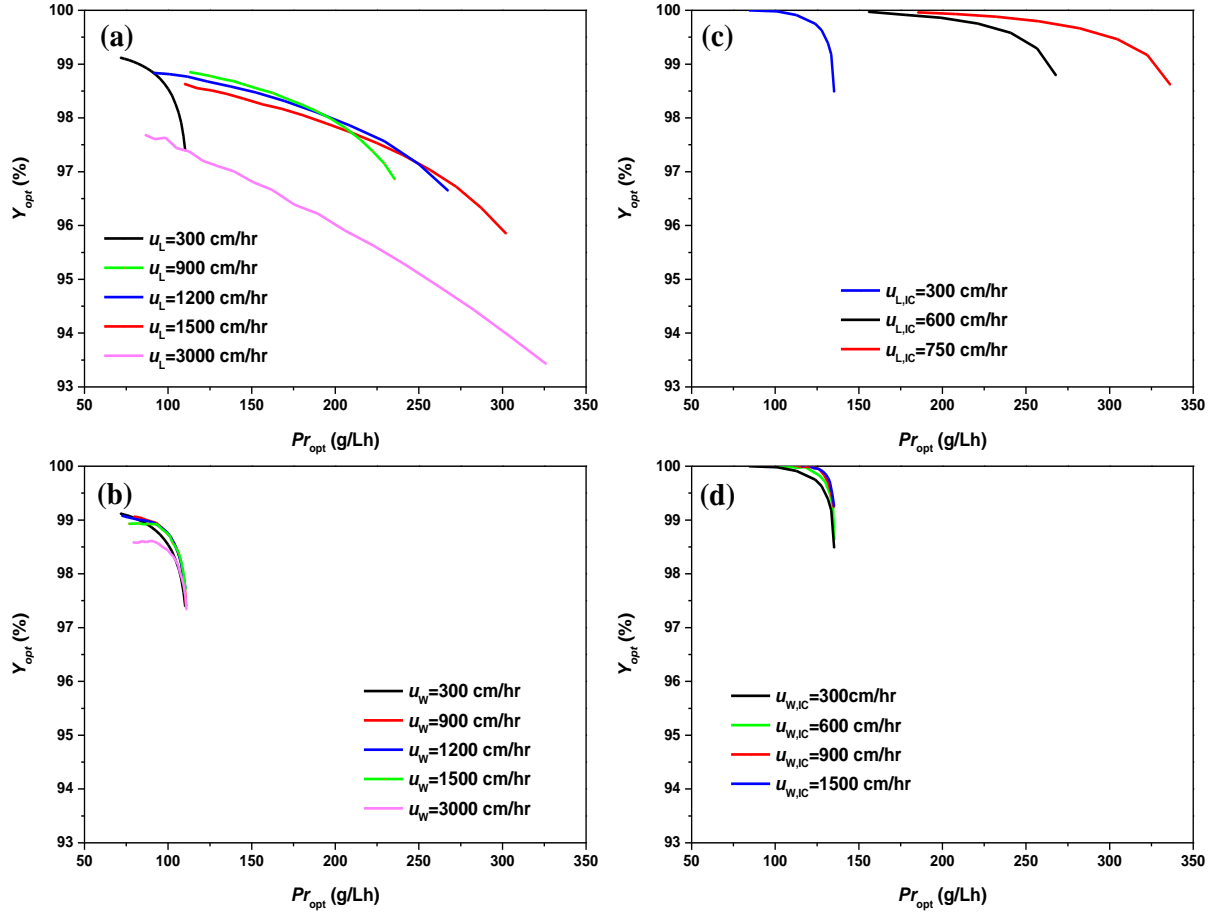
yield and productivity decrease.

Figure 5. Tradeoff (Pareto front) between yield and productivity of (a) batch process

under various loading velocities with u_W = 300 cm/hr (b) batch process under various

washing velocities with u_L = 300 cm/hr (c) Flow2 process under various interconnected

loading velocities with $u_{W,IC}$ = 300 cm/hr (d) Flow2 process under various

interconnected washing velocities with $u_{L,IC}$ = 300 cm/hr

Thus summarizing, since the Pareto fronts in both Figures 5a and 5b tend to cross

each other, the best velocity values have to be defined depending on the specific

operating conditions. In particular, the idea of using the maximum possible velocity in

368 either loading or washing, corresponding in this case to 3000 cm/hr, is not

369 recommended.

4.2.2 Continuous Flow2 process

371 The analysis of the role of liquid velocities in this case is more complex than for

372 batch processes because we now deal with four velocities: the interconnected loading

373 velocity, $u_{L,IC}$, the interconnected washing velocity, $u_{W,IC}$, the inline dilution velocity,

374 u_{ILD} and the batch loading velocity, $u_{L,B}$. It appears reasonable to take equal the batch

375 and interconnected loading velocities, i.e. $u_{L,IC} = u_{L,B}$, so as to apply in both the same

376 residence time. In addition, the inline dilution velocity is taken equal to the

377 interconnected washing velocity, i.e. $u_{W,IC}=u_{ILD}$ as the resulting buffer composition for

378 the downstream column remains constant independent of the linear velocity applied,

379 thereby reducing the number of varied operating variables. Accordingly, in the

380 following we analyze the effect of two velocities: $u_{L,IC}$ and $u_{W,IC}$. These will be changed

381 independently, one at a time, in the range 300 cm/hr to 1500 cm/hr. The latter

382 corresponds to the largest velocity compatible with the considered maximum pressure

383 drop of 0.15 MPa, and it is half of the one considered in the case of the batch process

384 because two columns are operated in series in the interconnected step. The simulation

385 results are shown in Figure 5c and 5d.

386 In Figure 5c it is seen that larger values of the loading velocity, $u_{L,IC}$ improve

387 significantly the tradeoff between yield and productivity of the Flow2 process. However,

388 no Pareto Front could be calculated for loading velocities larger than 750 cm/hr, since

389 it was not possible to achieve the requested purity of 99%. For such values of $u_{L,IC}$ (and

of $u_{L,B}$), together with the fact that the batch loading time must be fixed to match the R-R time, too many aggregates breakthrough into the product pool. Nevertheless, it is found that, although the loading velocity is constrained by time scheduling, the Flow2 process can offer better performances than the batch operation. In particular, it can approach productivities larger than 300 g/L/h while keeping the yield in the order of 99%, which for the batch process (Figure 5a) can only by achieved by decreasing the productivity by at least three times in the order of 100 g/L/h.

Also in the case of the washing step, the process performance improves for increasing linear velocity values, $u_{W,IC}$ as shown in Figure 5d. This is because in the Flow2 process, the inline dilution allows all proteins washed out from the first column to be captured by the second column, regardless of the more or less harsh washing conditions in the first column. Better performance can be achieved compared to the batch process in terms of both yield and productivity.

Thus concluding, for the Flow2 process we can recommend the higher loading and washing velocities compatible with the pressure drop constraint, provided that the P_{spec} is obtained (750 cm/hr and 1500 cm/hr, respectively in this work). This is the main reason for the continuous process to exhibit better productivities than the corresponding batch operation, thus over compensating for the increased column volume utilized.

4.3 Role of buffer composition in loading and washing

In this section, the effect of the ionic strength of the loading and washing buffers is investigated. Also in this case, we analyze the effect of each one separately, by keeping the other fixed. In particular, we consider the ionic strengths of the loading

buffer, I_L ranging from 40 mM to 120 mM, and for the washing buffer higher values, with I_W ranging from 80 mM to 200 mM. The values of the remaining operating parameters are summarized in Tables 1 to 3, and in particular the ionic strength for inline dilution buffer is kept constant at $I_{ILD} = 10$ mM.

4.3.1 Batch process

The Pareto fronts computed for various values of the ionic strength of the loading buffer, I_L and at fixed ionic strength of the washing buffer, I_W equal to 120 mM, are shown in Figure 6a. It is seen that the process performance improves as I_L decreases. Lower ionic strength values, in fact, facilitate the displacement of the monomer by the aggregates by enlarging the difference of adsorptivity between aggregates and monomer. Using equations 6, 7 and 8, it can be seen that the ratio of the Henry coefficients of aggregates and monomer (H_{agg}/ H_{mono}) increases from about 40 to 600, as I_L decreases from 120 to 40 mM. Therefore, lower ionic strengths of the loading buffer can increase the monomer content and decrease the aggregate content in the product pool of the loading step. This comes of course in addition to the fact that using lower I_L typically implies also higher feed dilution and therefore lower protein concentration in the feed.

With respect to the washing conditions, a non-monotonous behavior is observed in Figure 6b: the process performance initially improves with increasing the wash buffer ionic strength, but then deteriorates at higher values. In particular, at $I_W = 140$ mM the Pareto becomes minute, indicating that the specified purity value can be achieved only for a restricted range of yield and productivity values. The reason is that in the batch process, the washing buffer has to be carefully tuned in order to elute the

434   remaining monomer inside the column without eluting also the aggregates. Too low I_w

435   lead to too much monomer left in the column, thus decreasing yield and productivity,

436   while too high I_w increase the aggregate leakage, thus leading to lower product purities.
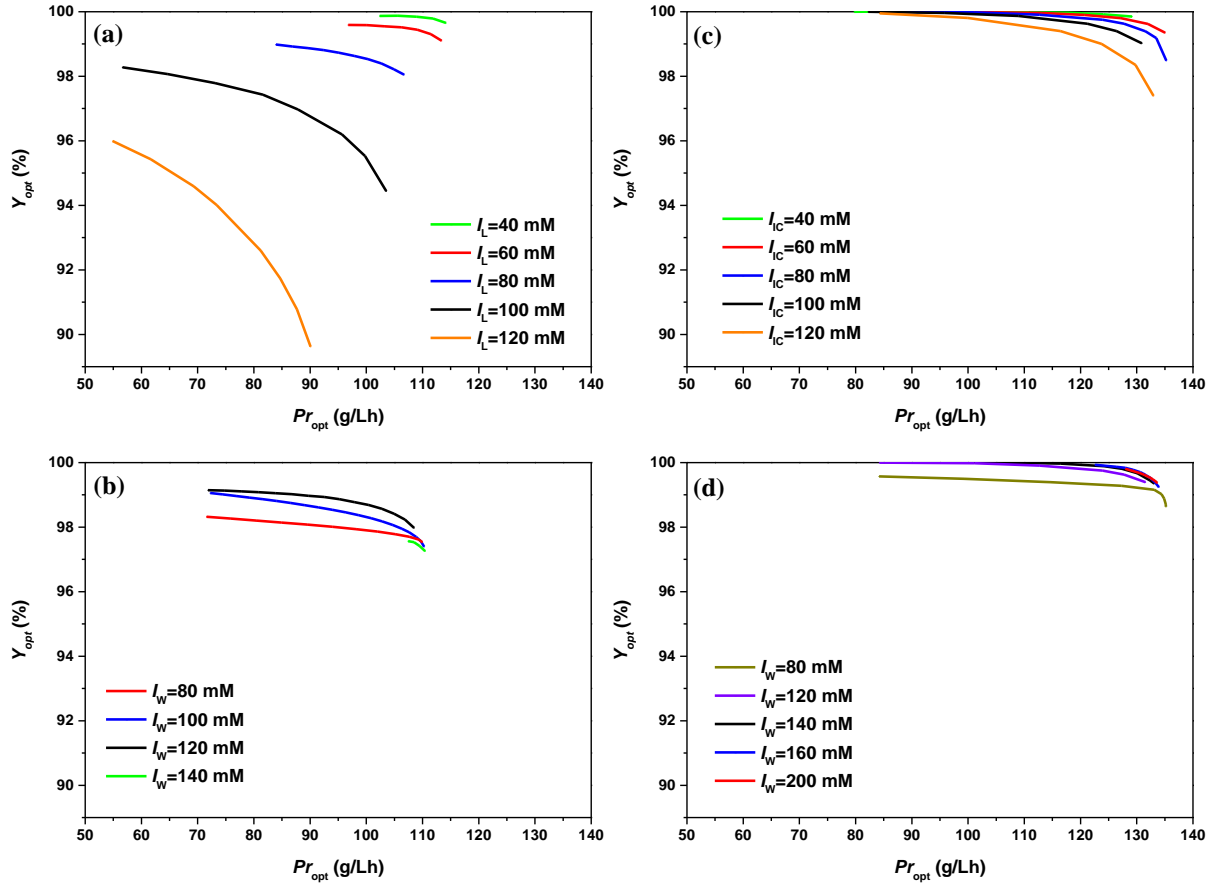
437

438   *Figure 6. Tradeoff (Pareto Front) between yield and productivity of (a) Batch process*

439   *for various ionic strengths of the interconnected loading buffer, I_L, with I_W = 120 mM.*

440   *(b) Batch process for various ionic strengths of the interconnected washing buffer, I_W,*

441   *with I_L = 80 mM.   (c) Flow2 process for various ionic strengths of the interconnected*

442   *loading buffer, I_{IC}, with I_W = 120 mM.   (d) Flow2 process for various ionic strengths*

443   *of the interconnected washing buffer, I_W, with I_{IC} = 80 mM.*

444   The conclusion of this analysis is that, for batch processes, while for the loading

buffer lower ionic strength values (40 mM in this work) are recommended, for the washing buffer a detailed analysis is needed to identify the proper ionic strength (120 mM in this work). The latter constitutes a delicate design problem, which obviously reflects at the manufacturing level in a control problem, which may have a strong influence on the performance of the entire process. This aspect will be discussed later in terms of process robustness.

4.3.2 Continuous Flow2 process

In the case of the Flow2 process we have four buffers involved and therefore four variables to be designed and optimized: the interconnected loading buffer ionic strength, $I_{L,IC}$, the batch loading buffer ionic strength, $I_{L,B}$, the interconnected washing buffer ionic strength, $I_{W,IC}$, and the inline dilution washing buffer ionic strength, I_{ILD}. In the following, I_B is set to be equal to I_{IC}, since, for practical reasons, it is convenient to use in both steps the same feedstock, coming from the protein A eluate and corrected to this ionic strength value. In addition, the I_{ILD} is set to be fixed at 10 mM, so that the Pareto optimization can be limited only to the interconnected loading buffer ionic strength, $I_{L,IC}$ and the interconnected washing buffer ionic strength, $I_{W,IC}$. Similarly as for the batch process, we investigate the process performance first for I_{IC} ranging from 40 to 120 mM at fixed I_W = 120 mM, and then for I_W changing from 80 to 200 mM at fixed I_{IC} = 80 mM. The obtained results are shown in Figures 6c and 6d, respectively.

In Figure 6c it can be seen that, similarly to the batch process, also for the Flow2 process the performance improves, that is the Pareto Front moves to the upper right corner of the plot, as I_{IC} decreases, although to a smaller extent. On the other hand, for

I_W, the data in Figure 6d show that the process performance first improves as the washing buffer ionic strength increases, but then reaches a kind of plateau for I_W values in the order of 140 to 200 mM where the process performance remains substantially unchanged. Besides providing in general better performances than the batch process, it is remarkable that this behavior of the Flow2 process is qualitatively different from that of the batch process, which indicates a superior robustness to changes in the washing buffer. In Figure 6b it can be seen, in fact, that the batch process for the largest values of I_W, from around 100 to 140 mM, undergoes tremendous changes in its performance. This indicates that the Flow2 process can tolerate larger changes in the washing buffer ionic strength without compromising the process performance, which instead drops substantially for the batch process. This higher robustness of the Flow2 process clearly originates from the higher process flexibility, and in particular by the inline dilution, which allows for the re-adsorption in the downstream column of the impurities desorbed in the upstream column, therefore preventing product pool contamination even at strong washing conditions.

To conclude, for the Flow2 process, lower ionic strength for the loading buffer, I_{IC} (40 mM in this work) and higher ionic strength for the washing buffer, I_W (higher than 160 mM in this work) are generally recommended to obtain best process performance in terms of both yield and productivity.

5 Process Robustness and Sensitivity Analysis

Robustness is an important factor when evaluating the performance of a process.

489   This is relevant at the process development stage, since higher robustness makes it

490   easier to identify operating conditions leading to optimal process performance, but it

491   matters also at the manufacturing scale, by facilitating the design of the controller

492   needed to reject possible disturbances and keep the process within specifications.

493   In this section, we address this issue through the process sensitivity analysis[37].

494 In particular, we define the normalized sensitivity, $S(\psi;\varphi)$ of the generic output process

495 parameter, ψ to small changes of the generic input process parameter, φ as follows:

496
$$S(\psi;\varphi) = \frac{\partial \psi}{\partial \varphi}\left(\frac{\varphi}{\psi}\right) \tag{13}$$

497 The partial derivative quantifies the local change of ψ with respect to a small change

498 of φ, *while keeping all remaining parameters constant*, and it is therefore appropriate

499 to estimate the sensitivity of the output, ψ with respect to the input, φ. The ratio φ/ψ

500 is introduced to make the sensitivity dimensionless, that is independent of the units used

501 in the evaluation of the input and output process parameters. However, it should be

502 noted that the normalized sensitivity values alone do not represent the output variability

503 due to a given imput parameter, since this is also affected directly by the intrinsic
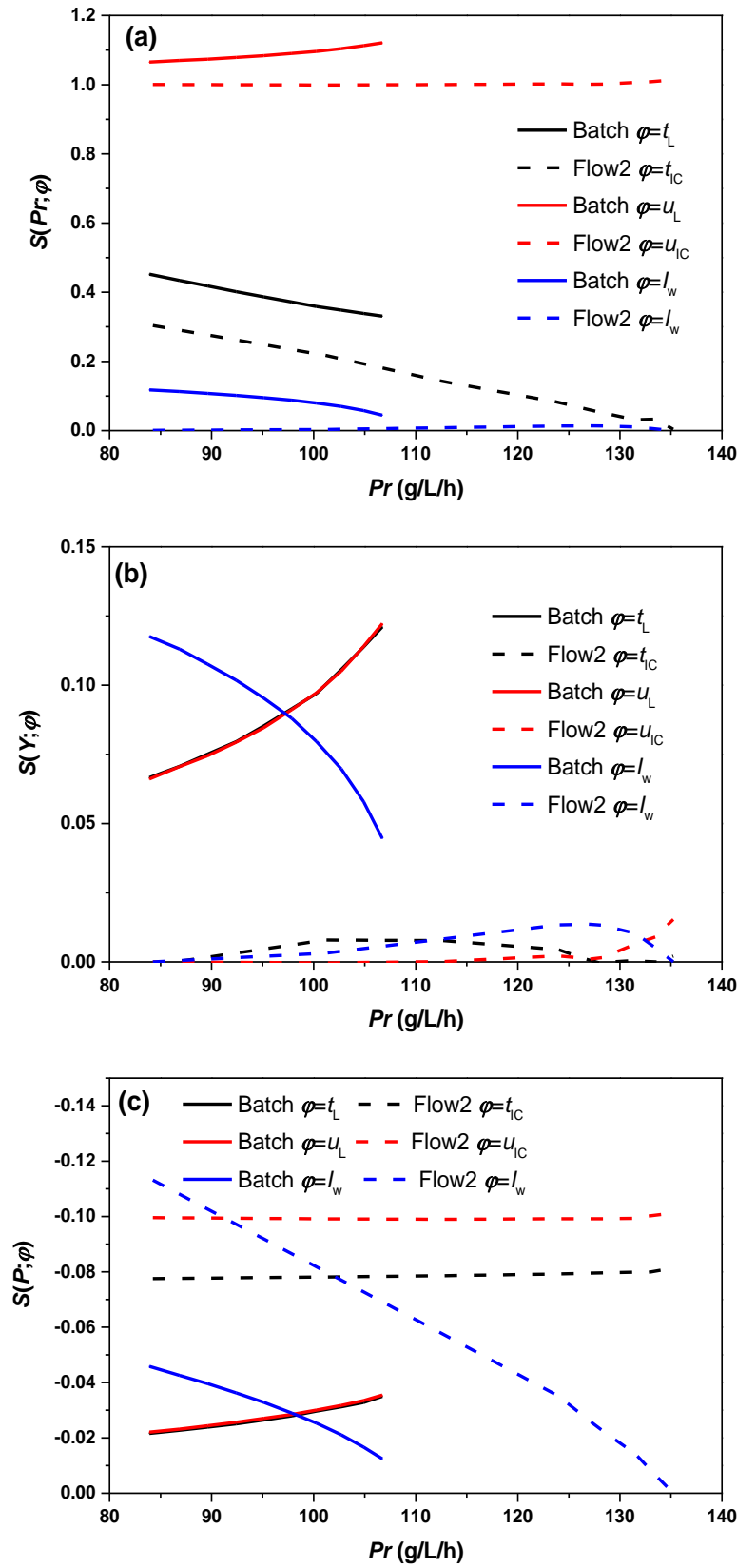
504 variability of the input parameter.

505 In the following, the sensitivity value is approximated through the incremental ratio

506 $((\psi(\varphi + \triangle \varphi) - \psi(\varphi))/\triangle \varphi)$, where the numerator represents the change in the

507 output parameter corresponding to an imposed change of the input parameter, equal to

508 +1% of the reference conditions considered in the sensitivity analysis. In particular, we

509 consider, as output process parameters, the three parameters determining the process

510 performance: productivity, yield and purity, that is $\psi = Pr$, Y and P, respectively. As

process input parameters we consider the loading time, the loading velocity and the

washing buffer ionic strength, that is $\varphi = t_L$, u_L and I_W, respectively.

As reference conditions for the sensitivity analysis we select the optimised

operating conditions along the Pareto fronts with $P_{spec} = 99\%$ shown in Figure 3 for the

batch and Flow2 process, respectively. Accordingly, for the various operating

conditions along the Pareto Front, we compute, for each given change in the input

parameter, the corresponding changes in the three performance parameters above, and

from these the corresponding sensitivity values through equation (13). The obtained

results, shown in Figure 7a to 7c, indicate that productivity and yield exhibit a *positive*

sensitivity value, while the the purity sensitivity is *negative*. This is consistent with the

fact that each of the considered operating conditions belong to the Pareto front at a fixed

purity value equal to 99%. The perturbed operating parameters, in fact, although leading

to improvements in productivity and yield (positive sensitivity value), lead to a lower,

not acceptable, purity value (negative sensitivity value) and therefore cannot be part of

the Paretoe Front. In the same Figure 7 it is also seen that the Flow 2 process, which

can achieve larger productivity values because of its higher efficiency, also exhibits a

generally better sensitivity behavior. More specifically, the very high sensitivity of the

yield with respect to the washing buffer ionic strength, I_w exhibited by the batch process

is largely removed in the Flow2 process.

In particular, Figure 7a shows that productivity is the most sensitive of all

considered output parameters, and the corresponding sensitivity values are substantially

equivalent for the two processes. Significantly lower sensitivity of the Flow2 process

533   is observed only for the washing buffer ionic strength, I_w and for the larger productivity

534   values. The strong reduction of the yield sensitivity with respect to I_w, mentioned above,

535   is illustrated in Figure 7b: The sensitivity values for the Flow2 process are less than

536   0.015, compared to values about ten times larger, in the order of 0.1, for the batch

537   process. This is a consequence of the stabilizing effect of the inline dilution process

538   discussed above in the context of Figures 6b and 6d. It is worth noting that, in Figure

539   7b, the yield sensitivities with respect to t_L and u_L for the batch process are almost

540   coincident. This is because these two parameters have the same effect on the loading

541   amount, which is in fact defined by their product, $(t_L * u_L)$, which in turns leads to the

542   same change in the yield value. The same observation applies to the purity sensitivities,

543   as it can be seen in Figure 7c. On the other hand, in Figure 7c, the batch process shows

544   lower purity sensitivities than the Flow2 process, with respect to any of the input

545   process parameters considered. However, the sensivities with respect to the loading

546   time and velocity are less critical in the context of process control (switching times and

547   flow rates are typically well controlled), and the observed differences are lower than in

548   the case above. On the other hand, the most critical sensitivity, with respect to I_w, can

549   be substantially decreased when operating at high productivity values.

550

Figure 7. Normalized sensitivity of productivity (a), yield (b) and purity (b) with respect

to t_L, u_L and I_W for the batch process and to t_{IC}, u_{IC} and I_W for the Flow2 process, along

the corresponding Pareto fronts shown in Figure 3.

6 Conclusion

Frontal chromatography has been analyzed with respect to two alternative implementations: a single column, batch process and a two-column, continuous process, referred to as Flow2. In particular, its application in the polishing step of the processes for mAb manufacturing, where the immunogenic high molecular weight species are removed from the target protein, is investigated with reference to a case of industrial relevance. An ad-hoc procedure for process optimization has been developed and validated through a general multiobjective optimization procedure, in terms of the Pareto Front of yield and productivity at a given purity, for both processes. The derived procedure allowed a thorough comparison of the two processes at their corresponding optimal operating conditions and not only in terms of the performance parameters, such as yield, purity and productivity, but also with respect to process robustness through a proper local sensitivity analysis.

The obtained results indicate that, although column interconnection puts constraints on the linear velocities of the Flow2 process, this in general achieves better performance in terms of both yield and productivity at a given purity, compared to the batch process. An important component of this improvement is the higher flexibility provided by the inline dilution process, which allows the Flow2 to better tolerate higher, and therefore more advantageous, ionic strength values in the washing step. The

comparison of the normalized sensitivities computed for the two processes shows that the Flow2 process exhibits much smaller yield sensitivities than the batch one. Even more importantly, it is shown that for the Flow2 process, optimal operating conditions can be found, where the process performance is not very sensitive to the washing conditions and in particular to the buffer ionic strength. This is a very important result, since this high sensitivity represents one of the largest drawbacks of the frontal chromatography batch process, which is the reason for its lack of robustness and reflects in difficulties in determining washing conditions that can guarantee reliable operation particularly at the large scale.

The discussed robustness analysis is based on the study of the *local* sensitivity values defined by equation (13). These local values are relevant, for example, for determining the characteristics of the algorithm used to control a specific input variable, e.g. determine the largest deviations that can be allowed to the input variable. It is interesting to note that the above reached conclusion is in good agreement with the analysis reported by Vogg et al. [18] based on a *global* definition of robustness. In particular, they compared the robustness of the two processes by considering the amplitude of the range of operating conditions, which allow respecting specific requirements in terms of process performance parameters. While their results indicate that the Flow2 process is characterized by larger robust design spaces than the batch process, our results augment this behavior by showing decreased local sensitivity of the Flow2 process towards process parameter variations at given sets of process parameters.

Notations

596

597   d_p Particle diameter (m)

598     $d_{ax,i}$ Axial dispersion coefficient of i component (m^2/s)

599   H_i Henry coefficient (atm*m^2/mg)

600   I_B Ionic strength of Batch loading buffer of Flow2 process (mM)

601   I_{IC} Ionic strength of Batch and Flow2 interconnected loading

602   buffer (mM)

603   I_L Ionic strength of Batch and Flow2 loading buffer (mM)

604   I_W Ionic strength of Batch and Flow2 washing buffer (mM)

605   I_{ILD} Ionic strength of Flow2 inline dilution buffer (mM)

606     $k_{m,i}$ Mass transfer coefficient of i component (m^2/s)

607   L_{col} Column length (m)

608   Pr Process Productivity (g/Lh)

609   P_i Purity for i component

610   P_{spec} Specification value for purity

611   u_L Batch loading linear velocity (mL/min)

612   u_W Batch washing linear velocity (mL/min)

613     $u_{L,IC}$ Flow2 interconnected loading linear velocity (cm/hr)

614     $u_{W,IC}$ Flow2 interconnected washing linear velocity (cm/hr)

615   u_{ILD} Flow2 inline dilution linear velocity (cm/hr)

616     $u_{L,B}$ Flow2 disconnected loading linear velocity (cm/hr)

617   q_i Concentration of i component in solid phase (mg/mL)

618   q_i^{eq} Equilibrium concentration of i component in solid phase

619   (mg/mL)

620   q_i^{sat} Saturation binding capacity of i component in solid phase

621   (mg/mL)

622   t_L Batch loading time (min)

623   t_w Batch washing time (min)

624   t_{RR} R-R time for batch and Flow2 process (min)

625    $t_{L,IC}$ Flow2 interconnected loading time (min)

626   u_{sf} Superficial velocity (m/s)

627   Y_i Yield for i component

628    $\varepsilon_{t,i}$ Total accessible porosity of I component

629   μ   Mobile phase dynamic viscosity (1.0 mPas)

630

References:

632 [1] H. L. Levine, J. E. Lilja, R. Stock, H. Hummel, S. D. Jones, *BioProcess Int* **2012**, *10*, 20.

633 [2] D. M. Ecker, S. D. Jones, H. L. Levine, *MAbs*, **2015**, 9.

634 [3] S. Singh, N. K. Tank, P. Dwiwedi, J. Charan, R. Kaur, P. Sidhu, V. K. Chugh, *Current clinical*
635 *pharmacology* **2018**, *13*, 85.

636 [4] H. Kaplon, J. M. Reichert, *MAbs*, Taylor & Francis **2019**, 219.

637 [5] A. L. Grilo, A. Mantalaris, *Trends Biotechnol.* **2019**, *37*, 9.

638 [6] S. S. Farid, J. Washbrook, N. J. Titchener Hooker, *Biotechnol. Progr.* **2005**, *21*, 486.

639 [7] C. A. Challener, *Biopharm Int.* **2014**, *27*, 20.

640 [8] S. Vogg, T. Muller-Spath, M. Morbidelli, *Current opinion in chemical engineering* **2018**, 22, 138

641 [9] F. Feidl, S. Vogg, M. Wolf, M. Podobnik, C. Ruggeri, N. Ulmer, R. Wälchli, J. Souquet, H. Broly,
642 A. Butté, Biotechnol. Bioeng. 2020, 117, 1367.

643 [10] D. J. Karst, F. Steinebach, M. Morbidelli, Curr. Opin. Biotech. 2018, 53, 76.

644 [11] FDA, Modernizing the way drugs are made: a transition to continuous manufacturing , **2017**.

645 [12] FDA, Quality consideratrions for continuous manufacturing-guidance for industry **2017**.

646 [13] G. Carta, A. Jungbauer, *Protein chromatography: process development and scale-up*, John Wiley
647 & Sons, **2020**.

648 [14] T. Ichihara, T. Ito, Y. Kurisu, K. Galipeau, C. Gillespie, *MAbs*, Taylor & Francis **2018**, 325.

649 [15] H. F. Liu, B. McCooey, T. Duarte, D. E. Myers, T. Hudson, A. Amanullah, R. van Reis, B. D. Kelley,
650 *J. Chromatogr. A* **2011**, *1218*, 6943.

651 [16] D. Pfister, L. Nicoud, M. Morbidelli, *Continuous Biopharmaceutical Processes: Chromatography,*
652 *Bioconjugation, and Protein Stability*, Cambridge University Press **2018**.

653 [17] M. T. Stone, K. A. Cotoni, J. L. Stoner, *J. Chromatogr. A* **2019**, *1599*, 152.

654 [18] S. Vogg, T. Müller-Späth, M. Morbidelli, *J. Chromatogr. A* **2020**, 460943.

655 [19] N. J. Titchener Hooker, P. Dunnill, M. Hoare, *Biotechnol. Bioeng.* **2008**, *100*, 473.

656 [20] S. L. C. Ferreira, R. E. Bruns, E. G. P. Da Silva, W. N. L. Dos Santos, C. M. Quintella, J. M. David,
657 J. B. de Andrade, M. C. Breitkreitz, I. C. S. F. Jardim, B. B. Neto, *J. Chromatogr. A* **2007**, *1158*, 2.

658 [21] C. Shi, Z. Gao, Q. Zhang, S. Yao, N. K. Slater, D. Lin, *J. Chromatogr. A* **2020**, 460936.

659 [22] N. Andersson, H. Knutson, M. Max-Hansen, N. Borg, B. Nilsson, *Ind. Eng. Chem. Res.* **2014**, *53*,
660 16485.

661 [23] T. Müller-Späth, G. Ströhlein, L. Aumann, H. Kornmann, P. Valax, L. Delegrange, E. Charbaut, G.
662 Baer, A. Lamproye, M. Jöhnck, *J. Chromatogr. A* **2011**, *1218*, 5195.

663 [24] D. Baur, M. Angarita, T. Müller Späth, M. Morbidelli, *Biotechnol J.* **2016**, *11*, 135.

664 [25] S. M. Pirrung, M. Ottens, *Preparative Chromatography for Separation of Proteins* **2017**, 269.

665 [26] T. Müller Späth, M. Krättli, L. Aumann, G. Ströhlein, M. Morbidelli, *Biotechnol. Bioeng.* **2010**, *107*,
666 652.

667 [27] J. Siitonen, M. Mänttäri, A. Seidel-Morgenstern, T. Sainio, *J. Chromatogr. A* **2015**, *1391*, 31.

668 [28] G. Guiochon, A. Felinger, D. G. Shirazi, *Fundamentals of preparative and nonlinear*
669 *chromatography*, Elsevier, **2006**.

670 [29] G. Carta, A. Jungbauer, Wiley-VCH Verlag GmbH, **2010**.

671 [30] B. Guélat, R. Khalaf, M. Lattuada, M. Costioli, M. Morbidelli, *J. Chromatogr. A* **2016**, *1447*, 82.

672 [31] G. Zames, N. M. Ajlouni, N. M. Ajlouni, N. M. Ajlouni, J. H. Holland, W. D. Hills, D. E. Goldberg,
673 *Information Technology Journal* **1981**, *3*, 301.

674 [32] https://it.mathworks.com/help/gads/gamultiobj.html, **2020**

675 [33] J. P. Abulencia, L. Theodore, *Fluid flow for the practicing chemical engineer*, Wiley Online Library,
676 **2009**.

677 [34]https://www.merckmillipore.com/Web-CH-site/de_DE/-/CHF/ShowDocument-
678 Pronet?id=201806.078, **2018**

679 [35] D. Farnan, D. D. Frey, C. Horváth, *Biotechnol. Progr.* **1997**, *13*, 429.

680 [36] G. Gotmar, T. Fornstedt, G. Guiochon, *J. Chromatogr. A* **1999**, *831*, 17.

681 [37] A. Varma, M. Morbidelli, *Parametric sensitivity in chemical systems*, Cambridge University Press,
682 **2005**.

683 [38] D. J. Downing, R. H. Gardner, F. O. Hoffman, *Technometrics* **1985**, *27*, 151.

684 [39] T. J. Krieger, C. Durston, D. C. Albright, *Transactions of the American Nuclear Society* **1978**, *28*.